LAWRENCE
LIVERMORE
NATIONAL
LABORATORY

UCRL-JRNL-200184

Taking X-ray Diffraction to the Limit: Macromolecular Structures from Femtosecond X-ray Pulses and Diffraction Microscopy of Cells with Synchrotron Radiation

J. Miao, H. N. Chapman, J. Kirz, D. Sayre, K. O. Hodgson

October 8, 2003

Annual Review of Biophysics and Biomolecular Structure

TAKING X-RAY DIFFRACTION TO THE LIMIT: MACROMOLECULAR STRUCTURES FROM FEMTOSECOND X-RAY PULSES AND DIFFRACTION MICROSCOPY OF CELLS WITH SYNCHROTRON RADIATION

Jianwei Miao,[1] Henry N. Chapman,[2] Janos Kirz,[3] David Sayre,[3] and Keith O. Hodgson[1,4]
[1]Stanford Synchrotron Radiation Laboratory, Stanford Linear Accelerator Center, Stanford University, Stanford, CA 94309-0210; [2]Lawrence Livermore National Laboratory, 7000 East Avenue, Livermore, California 94550; [3]Department of Physics and Astronomy, Stony Brook University, Stony Brook, NY 11794; [4]Department of Chemistry, Stanford University, Stanford, CA 94305;e-mail: miao@ssrl.slac.stanford.edu; chapman9@llnl.gov; kirz@xray1.physics.sunysb.edu; sayre@xray1.physics.sunysb.edu; hodgson@ssrl.slac.stanford.edu

Key Words the oversampling phasing method, iterative algorithms, diffraction microscopy, X-ray free electron lasers, single molecule imaging

Abstract

The methodology of X-ray crystallography has recently been successfully extended to the structure determination of non-crystalline specimens. The phase problem was solved by using the oversampling method, which takes advantage of "continuous" diffraction pattern from non-crystalline specimens. Here we review the principle of this newly developed technique and discuss the ongoing experiments of imaging non-periodic objects, like cells and cellular structures using coherent and bright X-rays from the 3rd generation synchrotron radiation. In the longer run, the technique may be applied to image single biomolecules by using the anticipated X-ray free electron lasers. Computer simulations have so far demonstrated two important steps: (i) by using an extremely intense femtosecond X-ray pulse, a diffraction pattern can be recorded from a macromolecule before radiation damage manifests itself, and (ii) the phase information can be *ab initio* retrieved from a set of calculated noisy diffraction patterns of single protein molecules.

CONTENTS

PERSPECTIVE AND OVERVIEW

X-ray crystallography yields high-resolution 3D images of molecules in the crystalline state, providing essential information in many areas of biology today. However, in important areas of molecular biology and throughout cell biology, structures of key biological interest exist which cannot currently be crystallized and are hence not accessible by conventional crystallography. An effort has therefore been underway for some years to extend the diffraction methodology employed in X-ray crystallography to the *general* small non-crystalline specimen, which we refer to as "X-ray diffraction microscopy". This approach, based primarily on the emergence of more powerful synchrotron X-ray sources, and on the presence of more favorable circumstances for dealing with the phase problem, is now looking promising, and is the subject of this review.

By "general small specimen" is meant a finite non-periodic isolated object of less than a few microns in size. This definition includes e.g. a single biomolecule, a cluster of biomolecules, an organelle, or a complete small cell. (Larger and non-isolated objects may also be possibilities for future study.) The objects covered closely resemble the objects covered by optical and electron microscopy. But, X-ray diffraction microscopy offers imaging resolution that is much higher than in the optical microscope and allows specimen thickness much higher than in the electron microscope.

In comparing diffraction microscopy with crystallographic imaging, the main difference is that the intensity of the diffraction signal is very much weaker in the non-crystalline case. This is due to the absence of the very large signal amplification which occurs at the Bragg peaks in the crystal case; that amplification can be of the order of N^2, where N is the number of unit cells in the crystal. This lowering of signal explains why the development of new X-ray sources is important for diffraction microscopy -- we are asking for the loss of Bragg-peak amplification to be made up for by the increase in source brightness. Fortunately, new sources of synchrotron radiation do appear to be capable of living up to that request. Equally important is a second condition, namely that the specimen used in diffraction microscopy be capable of withstanding a greatly intensified X-ray exposure. As will be seen, this, at least in the field of biological specimens, set the resolution limit of the technique.

The absence of Bragg-peak amplification also has an advantage: the observed diffraction pattern does not lose the information, which exists between the Bragg peaks. The favorable consequence of this is that the phase problem, difficult for the crystal specimen, becomes simpler for diffraction microscopy. More experience is needed, but indications are that phasing will not be a central problem for these types of experiments See Sec. 2 of the review.

Returning to the problem of the specimen withstanding of increased radiation exposure, there are two basic situations to be considered. In one, there is no crystal, but there exists a large supply of exact copies of the structure of interest, while in the other, exact copies do not exist. The first case is exemplified by a protein molecule, and is the more favorable in terms of the high-resolution quality of 3D imaging that can be envisioned; the second case is exemplified by a whole biological cell. In the first case the strategy can be to use a femtosecond flash X-ray source which will capture diffraction

data before the damage has had time to become evident, and expend many copies of the structure in the collecting of the full 3D dataset. In the second case, the strategy must be to employ measures, e.g. cryoprotection, to extend the lifetime of the specimen as much as possible during the 3D data collection in a high-brightness synchrotron X-ray beam. Detailed simulations indicate are that in the first scenario near atomic resolution imaging will be possible at least for relatively large macromolecules, while for the second scenario 10nm (or large-molecular) resolution may be possible. More detailed discussion of the second case will be found in Sec. 3, and of the first case in Secs. 4, 5, and 6.

Historically, work on the subject had its inception in the early 1980s at the Stony Brook physics department and the Brookhaven synchrotron (61). By 1990 it was established (78, 62) that pattern can be recorded from the general small specimen using synchrotron radiation. In 1995 an approximate treatment was given (63) of the relationship between dose and resolution, and by 1998 it was established (62, 64, 43) that with the gaining of information lying between Bragg peaks the phase problem is much reduced in difficulty. Finally, in 1999, Miao *et al*. (44) successfully demonstrated the complete procedure of pattern recording, phasing, and imaging, on a 2D man-made radiation-resistant specimen. Following this, other groups began to take up the subject (see references in later sections), and with this considerable research strength in the field has been brought into existence.

THE OVERSAMPLING PHASING METHOD AND ITERATIVE ALGORITHMS

The Principle of the Oversampling Method

The discovery of X-ray diffraction from crystals by von Laue in 1912 marked the beginning of a new era for visualizing the 3D atomic structures inside crystals. Indeed, after almost a century's development, X-ray crystallography has developed to a point that it can determine almost any structures, as long as good quality crystals are obtained. This remarkable achievement can be partially attributed to the development of powerful crystallographic phasing methods such as the direct methods (20), isomorphous replacement (21), molecular replacement (1), multiple wavelength anomalous dispersion (57, 28), and others (77). However, when the crystals become small or only have one unit cell (*i.e.* non-crystalline), the X-ray diffraction intensities are weak and continuous, and the crystallographic phasing methods can be improved upon. It turns out that, when the diffraction pattern is continuous, the phase information is much easier to recover by sampling the diffraction pattern at a spacing finer than the Bragg peak frequency (*i.e.* oversampling). It was first suggested by Sayre in 1952 that having the intensities between as well as at the Bragg peaks may provide the phase information (60). Bates proposed an explanation to the oversampling method in 1982 (2). Based on the argument that the autocorrelation function of any sort of object is twice the size of object itself in each dimension, Bates concluded that the phase information can only be recovered by sampling the intensities twice finer in each dimension than the Bragg peak frequency. In 1996, Millane further relieved Bates' criterion in three and higher dimensions (52).

In 1998, Miao, Sayre & Chapman proposed a different explanation to the oversampling method and concluded that Bates' criterion is overly restrictive (43). If

each intensity point is considered to be a nonlinear equation, which is related to the electron density in the specimen by the square of the magnitude of Fourier transform, solving the phase problem becomes how to solve this set of equations to recover the unknown electron density. When the intensities are sampled at Bragg peak frequency, there are exactly twice as many unknown as independent equations (47) where independent equations are defined as those intensity points having no crystallographic symmetry relationship. This is why, without any other information, the phases cannot be directly recovered from the diffraction pattern sampled at Bragg peak frequency. When the diffraction pattern is sampled at a spacing finer than the Bragg peak frequency, the number of independent equations increases while the number of unknown variables remains the same. We should point out that oversampling the diffraction pattern requires better coherence of the incident X-rays than Bragg sampling. The illumination needs to be both temporally (narrow bandwidth) and spatially (tight collimation) coherent (45, 46). This is because the higher the oversampling frequency, the finer the recording of the features in the diffraction pattern has to be. Equivalently, oversampling the diffraction pattern corresponds to surrounding the electron density with a no-density region, where the size of the no-density region is proportional to sampling frequency (47). An oversampling ratio was introduced to characterize the oversampling degree, which is defined as the ratio of the volume of the electron density and no-density region to the volume of electron density region (43). When the ratio is larger than 2, the number of independent equations is more than the number of unknown variables, and the phase information is in principle embedded inside the diffraction pattern. Having a larger number of independent equations than unknowns is a necessity, but not a guarantee to a unique solution. By using the theory of polynomials, it has been shown that, given noise-free diffraction pattern, there are usually $\leq 2^M$ multiple solutions in one dimension where M is the number of unknown variables (3, 11). But the multiple solutions are rare in two and three dimensions since 2D and 3D polynomials usually cannot be factorized.

Iterative Algorithms

Although in principle there exists a unique phase solution in an oversampled 2D or 3D diffraction pattern with the ratio larger than 2, it is not straightforward to find the solution (*i.e.* global minimum) from a large number of non-linear equations. One of the most effective ways is to use iterative algorithms. In 1972, Gerchberg & Saxton proposed a phase retrieval algorithm by iterating back and forth between real and reciprocal space (19). In real space an electron micrograph and in reciprocal space the diffraction pattern were used as constraints. In 1978, Fienup further improved the iterative algorithm by using the finite size of an object (*i.e.* support) and positivity as constraints in real space (16), where the positivity constraint is due to the fact that the electron density should be positive. Also independently, Stroud and Agard developed an iterative Fourier method in 1979 for the phase retrieval and refinement of 1D continuous diffraction pattern of membranes (70). While oversampling of continuous intensities in one dimension usually has multiple phase solutions as discussed above, a unique solution may be obtainable under certain conditions. In subsequent years, the shape of the finite support was thought to be critical to phasing a 2D and 3D diffraction pattern (16, 17). However, both simulation and experimental results suggested that the oversampling ratio is one of the

deterministic factors to the success of phase retrieval (43, 45). Recently Elser introduced a different algorithm for iterative phase retrieval, which he refers to as the "difference map" approach (15). In model calculations it has proven to be particularly powerful when the support constraint is poorly known, and when there is additional information about the specimen, such as atomicity or the spectrum of scattering strengths present in the form of a histogram. The iterative phase retrieval of complex-valued objects has also been pursued. By using tight support (17), enforcing positivity on the imaginary part of the objects (43) or applying more constraints such as histogram (35), correct phase information can usually be retrieved.

The iterative algorithms have now reached a point where the phase information can usually be reliably recovered from an oversampled diffraction pattern with reasonable signal to noise ratio. The algorithms, based on the Fienup approach (16), usually consist of the following four steps in each iteration (45).

(i). the magnitude of Fourier transform (*i.e.* square root of the measured diffraction intensities) is combined with the current best phase set. A random phase set is used for the first iteration.

(ii). Applying the inverse fast Fourier transform, a new electron density function is obtained.

(iii). Constraints are enforced on the electron density function. By pushing the electron density outside the support and the negative electron density inside the support close to zero, and retaining the positive electron density inside the support, a new electron density is defined.

(iv). Applying the fast Fourier transform to the new electron density, a new Fourier transform is calculated, resulting in a new set of phases. After setting the phase of central pixel to zero, this new phase set is used for the next iteration.

Note that there are other algorithms under development, which, while iterative, do not perform series of forward and inverse transforms. These efforts are extensions of methods used in crystallography, helped by the fact that they can now work on oversampled data. The first is the application of direct methods (69), and the second is a real-space conjugate-gradient minimization based on the EDEN program (23).

The combination of the oversampling method with iterative algorithms is gradually becoming a general and powerful phasing technique. It does not require resolution of the diffraction pattern at the atomic level and can solve large and complicated structures. While bearing some relationship with solvent flattering (73), non-crystallographic symmetry (10, 13, 59) and molecular replacement (1), the oversampling method does not need crystal samples and is an *ab initio* phase method. The generality of the oversampling method is due to the fact that the no-density region can be determined *ab initio*, and the size of the no-density region is proportional to the sampling frequency. However, its drawback is that the diffraction intensities are relatively weak. To carry out the experiments, it is necessary to use bright X-ray sources such as the 3rd generation synchrotron radiation and for imaging single biomolecules the future X-ray free electron lasers are required.

EXPERIMENTS USING SYNCHROTRON RADIATION

The possible extension of the methodology of X-ray crystallography to non-crystalline specimens (*i.e.* X-ray diffraction microscopy) was first suggested by Sayre in 1980 (61). While the concept is simple and elegant, the experiment itself is challenging in that the loss of crystallinity makes it difficult to record high quality diffraction pattern. In subsequent years, progress was made in recording diffraction patterns from non-crystalline specimens (78, 64). However, it was not until in 1999 that the first demonstration experiment was carried out by Miao *et al*. (44). Fig. 1A shows a test pattern made of a patch of Au dots on a silicon nitride membrane. The specimen was illuminated by coherent X-rays with a wavelength of 17 Å. Fig. 1B shows an oversampled diffraction pattern (450 x 450 pixels) with the oversampling ratio equal to 25. Due to a beamstop for blocking the direct beam, there were missing data in a 15-pixel-radius circle at the center, which were filled in by the intensities calculated from a lower resolution X-ray microscopy image (33). By using the iterative algorithm, the unique phase information was successfully retrieved, shown in Fig. 1C. Since then X-ray diffraction microscopy has been successfully applied to imaging a series of non-crystalline specimens and nano-crystals (48, 25, 45, 49, 58, 68, 72, 75, 38), in some cases even without the need to patch in missing data due to the beam stop. The 3D imaging of non-crystalline specimens using the oversampling phasing method has also been demonstrated recently, requiring the recording of a number of 2D diffraction patterns by rotating the specimen about one axis (46, 76).

The application to biological samples has also been pursued (50). The samples were *E. Coli* bacteria with manganese labeling of histidine-tagged yellow fluorescent proteins. The bacteria were air-dried and supported on a silicon nitride window. By using coherent X-rays with a wavelength of 2 Å from an undulator beamline at Spring-8, an oversampled diffraction pattern was recorded, shown in Fig. 2A. The intensities in an area of 70 x 70 pixels at the center were filled in by a patch of data calculated from a lower resolution X-ray micrograph. This oversampled diffraction pattern was directly converted to an image with a resolution of ~ 30 nm, shown in Fig. 2B. The reconstructed bacteria contain dense regions that probably represent the histidine-tagged proteins labeled with manganese and a semi-transparent region that is devoid of proteins. The observation was confirmed by both transmission and fluorescence microscopy images shown in Fig. 2C.

Looking forward, the methodology can in principle be applied to image whole cells and cellular structures in three dimensions, which are too thick for electron microscopy (5, 42). The resolution will be likely limited by radiation damage (26, 65, 39, see also Sec. 5). By cooling the samples down to liquid nitrogen or even liquid helium temperatures, previous X-ray experiments have shown that the radiation damage problem can be greatly reduced (40, 66). Indeed, the Stony Brook group has already embarked on the task of creating a 3D image of the yeast Saccharomyces cerevisiae. Since this task involves the collection of hundreds of diffraction patterns as the specimen is rotated, a special instrument was built (6). It incorporates a cryo-holder, so the frozen hydrated specimen can be kept at liquid nitrogen temperatures to minimize radiation damage. It also incorporates computer-controlled motorized stages to allow for the automation of alignment and rotation. Fig. 3 shows the diffraction pattern of a freeze-dried yeast cell obtained at the National Synchrotron Light Source, using this instrument. Since the experiment is highly demanding of coherent flux, data collection for 3D imaging will

take place at the brightest source of soft X-rays currently available, at Lawrence Berkeley Laboratory's Advanced Light Source.

FROM STORAGE-RING-BASED TO LINAC-BASED X-RAY SOURCES

Intense synchrotron sources play a key role in current and future diffraction microscopy experiments. The use of synchrotron radiation produced by electron storage rings was recognized and begun to be exploited in the seventies. Indeed, among the earliest and most dramatic demonstrations of the value of this extremely intense source of radiation were experiments carried out at Stanford on protein diffraction which clearly showed the value of both the high intensity (to obtain higher resolution diffraction patterns in much shorter time) (56) and the prospects for the use of anomalous dispersion to solve the phase problem (which has come to be known as MAD phasing) (57). While these early studies showed significant promise, it took more than a decade for synchrotron radiation to come into more routine use for macromolecular crystallography as well as biological small angle and x-ray absorption studies. This was due in part to the sources themselves (in particular lack of reliable operation early in their history) and as well as the instrumentation available at that time (*e.g*. no electronic data recording media for diffraction patterns). The early generation of storage rings was initially derived from those used for high-energy physics ("first" generation) and evolved and more optimized for synchrotron radiation production ("second" generation). Nonetheless, during the eighties and into the nineties, the most challenging structural biology problems were often addressed using synchrotron x-rays. As the sources themselves became much more reliable, and effective instrumentation was developed for taking measurements, there began a strong move toward using synchrotron radiation for x-ray based studies in structural biology (74).

In the nineties, a new class of synchrotron sources began to come online. These machines, called "third generation" sources, had lattices that were optimized for accepting insertion devices called undulators. Undulators provide a much narrower opening angle of radiation in which constructive interference effects dramatically increase the brightness. This can be seen graphically in Fig. 4, where the third generation sources are on average 10^4 higher brightness that available from the second generation ones. This higher brightness enabled more challenging experiments - pushing the boundaries to smaller crystal size, lower concentrations, faster times (for time resolved studies) and smaller spatial resolution. Today there are around 50 second and third generation synchrotron facilities around the world, a large number of which serve very active communities doing structural biology research.

There are ultimately limitations to the performance of storage rings, both in terms of brightness and also the length of the electron pulses (which generate the x-rays upon having their trajectories bent in bending magnets or insertion devices). Limitations on brightness come from the fact that the electron beam size is increased by the natural process of generation of synchrotron radiation. This effect can be reduced by larger circumference rings, with ultimately the "limit" being a straight line (that is a linear accelerator where there is no emission of synchrotron radiation to "spoil" the beam size and emittance). The nature of RF acceleration in storage rings also gives rise to a natural bunching of the electrons which have typical bunch lengths of a few hundred picoseconds

and except for some special laser based slicing techniques, cannot be reduced much below this value. This is illustrated graphically in Fig. 4 where it can be seen to first approximation that both the second and third generation synchrotron sources have similar pulse lengths.

It was recognized in the eighties and early nineties that linacs could be interesting and potentially revolutionary sources of synchrotron radiation. Electrons, being charged particles, can be quite easily manipulated; for example, they can be compressed along their direction of travel by chirping the beam in energy (that is introducing a spread in energy from the head to the tail of the bunch) and passing the chirped beam through a magnetic compressor (which bends the particles) where the high energy particles travel a shorter path than the low energy ones. Since the properties of the electron beam in linacs are directly determined by the source (rather than the equilibrium dynamics of the storage beam lattice), higher brightness electron guns offer the possibility of much smaller, lower emittance beams**.** The work on photo-cathodes as bright electron sources carried out mostly at Los Alamos National Laboratory in the eighties provided just the type of sources needed for Free-Electron Lasers. The ability to transport and accelerate such beams was developed by the accelerator physics community in work related to a next generation of high-energy physics machines called linear colliders. The combination of linac-based light sources with high performance insertion devices forms the basis for concepts of a next generation (the "fourth") of synchrotron light sources.

One implementation of linac based light sources is the energy recovery linac (ERL) where the energy of the electron beam remaining after it has passed through a series of undulators is recovered (71). This results in much improved operational efficiency. Such a concept operating at relatively low energies has been tested at the Thomas Jefferson National Accelerator Facility and has been proposed as a new x-ray source at Cornell University (22). Since the properties of the electron beam are primarily determined by the electron source (a high brightness photocathode gun), such an ERL can have much higher peak brightness with about a thousand fold shorter pulse length (see Fig. 4). While ERLs operating in the x-ray regime remain in the conceptual design stage, a linac-based light source based upon a single pass linac has recently become operational. The subpicosecond pulsed source (SPPS) at the Stanford Linear Accelerator Center (SLAC) utilizes a 28 GeV electron beam from the SLAC linear accelerator passed through a 2.5 m long undulator to produce a 80 femtosecond pulsed x-ray beam with more than 10^7 photons per pulse (see http://www-ssrl.slac.stanford.edu for details) (12).

High performance linacs combined with insertion devices offer yet another possibility to obtain even higher brightness x-ray beams. Madey first described the concept of low-gain free-electron lasers in the early seventies (37) and the concept of operation in a high gain limit (with single pass) was put forward somewhat later (8). Subsequently, Pellegrini proposed the idea of an x-ray free electron laser that would be based upon high energy electrons delivered by the SLAC linac and passed through a long (ca. 100 m) undulator (55). Such an XFEL, which has come to be known as the Linac Coherent Light Source (LCLS) has progressed from idea to design study and into detailed engineering and design. If funded by the U.S. Department of Energy on the anticipated schedule, LCLS will produce the world's first x-ray light in 2008 (see http://www-ssrl.slac.stanford.edu/lcls). A conceptually similar project is being planed at DESY in

Hamburg (the TESLA XFEL) and is expected to be operational in the 2011-2012 time frame (see http://www-hasylab.desy.de).

The photon properties of the LCLS will be remarkable as seen in Fig. 4. The high gain results in an increased peak brightness over the SPPS or planned ERLs by about 10^8. The x-rays produced by LCLS will be fully transversely coherent. The pulse length, initially in the range of 100-200 femtoseconds, can be shortened to below 100 fsec and with additional R&D it is expected to approach 1 fsec. Such extremely high brightness, short pulse and coherent x-rays have the potential to enable revolutionary experiments in biology. Such applications are considered below in extending X-ray diffraction microscopy to image single biomolecules.

OVERCOMING THE RADIATION BARRIER USING FEMTOSECOND X-RAY PULSES

As described in the previous sections, the ultimate resolution of X-ray diffraction microscopy for biological specimens is limited by radiation damage. Although the diffraction pattern is formed by elastically scattered particles, for every elastically scattered particle there are particles that deposit significant energy in the sample and hence cause damage (26). In the case of 12 keV x-rays, the dominant interaction with atoms is photoabsorption which, for low-Z atoms (such as C, N, O), occurs 10 times more often than elastic scattering (29). The absorption of a photon leads to a string of events, initiated by ejection of a *K*-shell (inner core) photoelectron. The atom relaxes in about 2 to 10 fs, primarily by emission of an Auger electron with an energy in the range of 250 to 500 eV (41). The subsequent cascade of collisional ionizations by the photo- and Auger electrons deposits half the initial energy of the x-ray photon into a roughly spherical volume on the order of about 1 micron diameter (for diamond), in about 6 fs, as determined by Monte Carlo simulation (80, 81). (The cascade takes about 100 fs to fully deposit all the initial energy.) This further leads to the breaking of chemical bonds, the excitation of vibrational modes of the material in 1–10 ps (53), and, in the absence of cryogenic cooling, diffusion or mass loss of the sample (7). Empirical estimates for the maximum steady-state dose in cryo-protected samples that does not cause morphological change at the atomic scale range from 10^8 to 10^{10} Gray (27, 66, 40, 39). This dose range corresponds to incident fluences of 2 to 200 photons/Å^2 for a protein sample exposed to 12 keV x-rays.

A way of overcoming the degrading effects of radiation damage is to record the diffraction pattern in a shorter time than the time of the damage process itself. Solem and colleagues (67) first suggested this idea of flash imaging as a way to overcome degradation of x-ray images of living wet cells and hydrodynamics calculations predicted that picosecond pulses could achieve about 10 nm resolution (36). These models assumed molecular thermalization processes at the 1 to 10 ps timescale and were not appropriate for modeling behavior at shorter times and higher resolution. However, a new understanding of the damage problem came with the detailed molecular dynamics analysis of Neutze *et al.* (54), which gave the first insight that atomic resolution could be possible using femtosecond pulses from an x-ray free-electron laser. This work also pointed out that there is another mechanism helping to reduce the effects of damage with short pulses, namely that using a short pulse enables injected or “containerless” samples

to be flash imaged. In this case, depending on sample size (79, 80, 81), the photoelectrons and possibly some Auger electrons will escape the sample and hence not initiate the damage reactions. This effect does however lead to an ever more positively charged sample as the exposure progresses, which leads to an inertia-limited Coulomb explosion that causes the eventual disintegration of the particle. The molecular dynamics calculations of Neutze *et al.* were based on a stochastic model of photoionization and Auger emission, and inelastic scattering. In small time steps, the ionization state of every atom was calculated, from which the equations of motion of all atoms are solved. The results showed that at pulse durations of 50 fs the tolerable incident fluence increases from the steady state value of 200 ph/Å^2 to 10^6 ph/Å^2, and to 10^7 ph/Å^2 for 5 fs pulses. At these exposures it was estimated that atomic resolution could indeed be achieved, especially for larger objects such as a single virus capsid.

In the work of Neutze *et al.* the photoelectrons and Auger electrons were assumed to leave the particle without further interaction, and it was noted that in actuality they would eventually be trapped. This has the effect of neutralizing the molecule and slowing down the Coulomb explosion at the expense of raising the temperature of free electrons in the molecule, causing a greater rate of ionization of atoms. Such effects have been considered in greater detail in two works: one with a Monte Carlo treatment of electrons interleaved with molecular dynamics steps (32), and another with a new hydrodynamic model (24). The two models appear to give quite similar results, with an advantage of the hydrodynamic model being that it is not limited to small (30-Å diameter) clusters of single atomic species. However, the hydrodynamic model assumes spherical symmetry and is only accurate in an average sense. In the hydrodynamic model the free electrons and ions are treated as two separate fluids that interact through the Coulomb force and ionization processes (described by time-dependent rate equations). It is found that although early on in the exposure some Auger electrons and most photoelectrons escape, the Auger electrons start becoming trapped after about <1 to 2 fs. Also the photoelectrons become trapped after about 10 fs if the particle is large (~>100 Å diameter). Since trapped electrons lead to further unbound electrons through collisional ionization, these cascades quickly dominate the damage process. It is also found that the trapped electrons quickly relax in energy and position to form a cloud around the positive ions, leaving a neutral core and a positively charged outer shell (similar to Debye shielding). The ion motion therefore peels off from the outer shell. In the inner core there is hardly any ion motion but the high electron temperature leads to a great amount of ionization and blurring of the electron density. It is this latter effect that requires pulse lengths of 10 fs or less to overcome damage with pulse fluences greater than 10^6 ph/Å^2. However, these limits might be relaxed if it were possible to reconstruct atomic positions from partially ionized atoms.

The damage models described above determine the degradation to structure at a given spatial scale, for a particular sample size, and pulse fluence (or sample dose) and duration. These models do not tell us what image resolution is achievable in a final reconstruction, which requires an analysis of the particular type of diffraction experiment.

POTENTIAL OF IMAGING SINGLE PROTEIN MOLECULES

One of the current bottlenecks in structural molecular biology is the difficulty of crystallizing protein molecules. Membrane proteins pose a particular challenge in this regard, and as a result only relatively a small number of structures of this important class have been determined. There are two established techniques to determine structure without crystals: NMR and single particle imaging using cryo electron microscopy. However, to date NMR can only solve the structures of relatively small protein molecules, and single particle imaging using cryo-electron microscopy has been limited to a resolution of ~ 10 Å for the asymmetrical ribosome (18) and ~ 6 - 7 Å for highly symmetrical viruses (9).

One approach, the combination of the oversampling phasing method with femtosecond X-ray pulses, may have the potential to overcome the obstacle (67, 54). To explore the hypothesis, a computer simulation has been carried out by using a rubisco protein molecule with molecular mass of 106,392 Da (51). The atomic coordinates were obtained from the Protein Data Bank (2RUB). The rubisco molecule was "illuminated" by a simulated X-ray free electron laser with a wavelength of 1.5 Å and a pulse of 2 x 10^{12} photons. The pulse duration was assumed to be short enough so that radiation damage could be ignored (see Sec. 5). Fig. 5 shows a schematic layout of a potential experimental set-up. The simulated X-ray laser was focused down to a 0.1 μm spot, for a pulse fluence of 2.55 x 10^6 ph/Å^2. The molecules were "dropped" into the beam in random orientation one at a time by a molecular spraying gun. In the simulation, each molecule was assumed to be hit by an X-ray pulse, and a total of 10^6 2D diffraction patterns were obtained from the identical rubisco molecules. The oversampled 2D diffraction patterns were assembled to an oversampled 3D diffraction pattern (160^3 voxels) with the assumption that the orientation of each molecule (and hence the 2D diffraction pattern) was known. To simulate a beamstop, the data in the central 3 x 3 x 3 voxels were removed. The molecule transform was then added Poisson noise with R = 9.7% where the R factor was used to characterize the difference between the noise-free molecule transform and the noisy one. By using the oversampling phasing method, the phasing information was *ab initio* retrieved from the 3D diffraction pattern. Fig. 6B shows the reconstructed electron density map of the active site which is in a good agreement with the same map obtained from the Protein Data Bank (Fig. 6A). To study the effect of phase retrieval as a function of noise, higher Poisson noise was added to the 3D diffraction pattern with R = 16.6%, where 3 x 10^5 identical molecules were used for the calculation. Fig. 6C shows the reconstructed 3D electron density of the active site.

While the computer simulation demonstrated the potential of imaging single molecules by combining the oversampling method with femtosecond X-ray pulses, it made two favorable assumptions: (i) radiation damage can be circumvented by using femtosecond X-ray pulses and (ii) the molecular orientation can be precisely determined. So far the computer modeling seems to support to the first assumption (see Sec. 5), and a real test has to wait for the availability of X-ray free electron lasers. The determination of molecular orientation could be carried out by two methods. One is to determine the molecular orientation from a series of 2D diffraction patterns, which has already been developed in single particle imaging using cryo-electron microscopy (14, 18). The other is to use a laser field to physically align each molecule before the exposure (34). With regard to the first method, a detailed statistical analysis has been performed that determines the signal levels required to be able to classify diffraction patterns of

randomly oriented particles (30). It is found that at the highest resolution, where the signal is weakest and the orientation determination is the most stringent, classification can be performed with signal levels below one photon per pixel. In general, for a given incident intensity and desired resolution, patterns from larger particles are easier to classify not only because they scatter more, but because there are more independent pixels to perform the correlation on. It is found that at fluences of 2×10^6 ph/Å^2 it is possible to classify patterns of 100-Å diameter molecules at a resolution better than 3 Å. At this intensity, as was discussed in the previous section, it should be possible to record diffraction patterns at this resolution with ~10 fs pulses.

SUMMARY AND OUTLOOK

X-ray diffraction microscopy, a combination of coherent and bright X-rays with the oversampling phasing method, is a newly developed methodology that makes it possible to escape the "benevolent tyranny" of the crystal in the reconstruction of structure from diffraction data (31). Due to the loss of the amplification from a large number of unit cells inside crystals, the major limitation of the application to structural biological seems to be radiation damage. By using cryo technologies, radiation damage can be significantly reduced, which makes it possible to image cells and cellular structures using X-ray diffraction microscopy. If with the planned femtosecond pulsed X-ray lasers, a 2D diffraction pattern can be recorded from a biomolecule before it is destroyed, this technique could open a new horizon of imaging protein molecules without the need of crystallizing them first.

ACKNOWLEDGEMENTS

We gratefully acknowledge our respective collaborators including Tetsuya Ishikawa, Yoshinori Nishino, Carolyn Larabell, Mark LeGros, Dan Durkin, Tobias Beetz, Chris Jacobsen, Enju Lima, David Shapiro, Stefan Hau-Riege, Richard London, Abraham Szöke, Stefano Marchesini, Alex Noy, Malcolm Howells, John Spence, Haifeng He, Janos Hajdu and Gösta Huldt. This work was supported by the U.S. Department of Energy, Office of Basic Energy Sciences. Additional support was provided by the US DOE Office of Biological and Environmental Research and the National Institutes of Health. Part of this work was performed under the auspices of the U. S. Department of Energy by University of California, Lawrence Livermore National Laboratory under Contract No. W-7405-ENG-48. Use of the RIKEN beamline (BL29XUL) at SPring-8 was supported by RIKEN.

LITERATURE CITED

1. Argos P, Rossman MG. 1980. Molecular replacement method. In Theory and Practice of Direct Methods in Crystallography, ed. MFC Ladd, RA Palmer, pp. 361-417. New York: Plenum.
2. Bates RHT. 1982. Fourier phase problem are uniquely soluble in more than one dimension. I: underlying theory. *Optik* 61:247-62.

3. Barakat R, Newsam G. 1984. Necessary conditions for a unique solution to two-dimensional phase recover. *J. Math. Phys.* 25:3190-3.
4. Barletta WA, Winick H. 2003. Introduction to special section on future light sources. *Nucl. Instr. And Meth*. A 500:1-10.
5. Baumeister W, Grimm R, Walz J. 1999. Electron tomography of molecules and cells. *Trends Cell Biol.* 9:81-5.
6. Beetz T., Jacobsin C, Kao CC, Kirz J, Mentes O, et al. 2003. Development of novel apparatus for experiments in soft X-ray diffraction imaging and diffraction tomography. *J. Phys. IV France.* 104:27-30.
7. Beetz T, Jacobsen C. 2002. Soft x-ray radiation damage studies in PMMA using a cryo-STXM. *J. Synch. Rad.* 10:280-283.
8. Bonifacio R, Pellegrini C, Narducci LM. 1985. Collective Instabilities and High Gain Regime in a Free-Electron Lasers. Opt. Commun. 50:373.
9. Bottcher B, Wynne SA, Crowther RA. 1997. Determination of the fold of the core protein of hepatitis B virus by electron cryomicroscopy. *Nature* 386:88-91.
10. Bricogne G. 1974. Geometric Sources of Redundancy in intensity data and their use for phase determination. *Acta Crystallogr.* A 30:395-405.
11. Bruck YM, Sodin LG. 1979. On the ambiguity of the image reconstruction problem. *Opt. Commun.* 30:304-8.
12. Cornacchia M. A et al. Sub-Picosecond Photon Pulse Facility for SLAC. *SLAC-PUB-8950*.
13. Crowther RA. 1969. The use of non-crystallographic symmetry for phase determination. *Acta Crystallogr.* B 25:2571-80.
14. Crowther RA. 1971. Procedures for three-dimensional reconstruction of spherical viruses by Fourier synthesis from electron micrographs. *Philos. Trans. Roy. Soc. Lond*. B. 261:221-30.
15. Elser V. 2003. Phase retrieval by iterated projections. *J. Opt. Soc. Am.* A 20:40-55.
16. Fienup JR. 1978. Reconstruction of an object from the modulus of its Fourier transform. *Opt. Lett.* 3:27-9.
17. Fienup, JR. 1987. Reconstruction of a complex-valued object from the modulus of its Fourier transform using a support constraint. *J. Opt. Soc. Am. A* 4:118-23.
18. Frank J. 2002. Single-particle imaging of macromolecules cryo-electron microscopy. *Annu. Rev. Biophys. Biomol. Struct.* 31:303-19.
19. Gerchberg RW, Saxton WO. 1972. A practical algorithm for the determination of phase from image and diffraction plane pictures. *Optik* 35:237-46.
20. Giacovazzo C. 1998. *Direct phasing in crystallography*. New York: Oxford University Press.
21. Green DW, Ingram VM, Perutz MF. 1954. The structure of haemolglobin IV. Sign determination by the isomorphous replacement method. *Proc. R. Soc. London Ser. A* 255:287-307.
22. Gruner SM, Tigner M, 2001. Study for a proposed Phase I Energy Recovery Linac (ERL) Synchrotron Light Source at Cornell University, *CHESS Technical MEMO 01-003 and JLAB-ACT-01-04*.
23. Hau-Riege SP, Szöke H, Chapman HN, Szöke A. 2003. SPEDEN: reconstructing single particles from their diffraction patterns. *J. Struct. Biol.* Submitted.

24. Hau-Riege SP, London RA, Szöke A. 2003. Dynamics of biological molecules irradiated by short x-ray pulses. Submitted to *Phys. Rev. E.*
25. He H, Marchesini S, Howells M, Weierstall U, Chapman H, Hau-Riege S, Noy S, Spence JCH. 2003. Inversion of X-ray diffuse scattering to images using prepared objects. *Phys. Rev.* B 67:174114.
26. Henderson R. 1995. The potential and limitations for neutrons, electrons and X-rays for atomic resolution microscopy of unstained biological molecules. *Q. Rev. Biophys.* 28:171-93.
27. Henderson R. 1990. Cryoprotection of protein crystals against radiation damage in electron and X-ray diffraction. *Proc. Roy. Soc. Lond. B* 241:6-8.
28. Hendrickson WA, Smith JL, Sheriff S. 1985. Direct phase determination based on anomalous scattering. *Meth. Enzymol*. 115:41-55.
29. Henke BL, Gullikson EM, Davis JC. 1993. X-ray interactions: photoabsorption, scattering, transmission, and reflection at E=50-30000 eV, Z=1-92. *At. Data Nucl. Data Tables* 54:181-342.
30. Huldt G, Szöke A, Hajdu J. 2003. Diffraction imaging of single particles and biomolecules. Submitted to *J. Struct. Biol.*
31. Johnson LN, Blundell TL. 1999. Introductory overview. J. Synchrotron Rad. 6:813-5.
32. Jurek Z, Faigel G, Tegze M. 2003. Dynamics in a cluster under the influence of intense femtosecond hard x-ray pulses. Submitted to *Phys. Rev. B.*
33. Kirz J, Jacobsen C, Howells M. 1995. Soft X-ray microscopes and their biological applications. *Q. Rev. Biophys.* 28:33-130.
34. Larsen JJ, Hald K, Bjerre N, Stapelfeldt H, Seideman T. 2000. Three Dimensional Alignment of Molecules Using Elliptically Polarized Laser Fields. *Phys. Rev. Lett.* 85:2470-3.
35. Lima E, Shapiro D, Kirz J, Sayre D. 2003. Algorithmic image reconstruction using iterative phase retrieval schema. *J. Phys. IV France.* 104:631-4.
36. London RA, Rosen MD, Trebes JE. 1989. Wavelength choice for soft x-ray laser holography of biological samples. *Appl. Opt.* 28:3397-3404.
37. Madey JM. 1971. *J. Appl. Phys.* 42:1906.
38. Marchesini S, He H, Chapman HN, Hau-Riege SP, Noy A, Howells MR, Weierstall U, Spence JCH. 2003. X-ray imaging without lenses. *Phys Rev. B* (in press).
39. Marchesini S, Chapman HN, Hau-Riege SP, London RA, Szöke A, He H, Howells MR, Padmore H, Rosen R, Spence JCH, Weierstall U. 2003. Coherent x-ray diffractive imaging: applications and limitations. Submitted to *Opt. Express.*
40. Maser J, Osanna A, Wang Y, Jacobsen C, Kirz, J, et al. 2000. Soft X-ray microscopy with a cryo STXM: I. Instrumentation, imaging, and spectroscopy *J. Microsc.* 197:68-79.
41. McGuire EJ. 1969. K-Shell Auger transition rates and fluorescence yields for elements Be-Ar. *Phys. Rev.* 185:1-6.
42. McIntosh JR. 2001. Electron Microscopy of Cells: A New Beginning for a New Century. *J. Cell Biol.* 153:25-32.
43. Miao J, Sayre D, Chapman HN. 1998. Phase retrieval from the magnitude of the Fourier transforms of non-periodic objects. *J. Opt. Soc. Am.* A 15:1662-69.

44. Miao J, Charalambous P, Kirz J, Sayre D. 1999. Extending the methodology of X-ray crystallography to allow imaging of micrometer-sized non-crystalline specimens. *Nature* 400:342-4.
45. Miao J, Ishikawa T, Anderson EH, Hodgson KO. 2003. Phase retrieval of diffraction patterns from non-crystalline samples by using the oversampling method. *Phys. Rev. B* 67:174104.
46. Miao J, Ishikawa T, Johnson B, Anderson EH, Lai B, Hodgson KO. 2002. High Resolution 3D X-ray Diffraction Microscopy. *Phys. Rev. Lett.* 89:088303.
47. Miao J. Sayre D. 2000. On possible extensions of X-ray crystallography through diffraction-pattern oversampling. *Acta Cryst*. A56:596-605.
48. Miao J, Kirz, J, Sayre, D. 2000. The oversampling phasing method. *Acta Cryst.* D56:1312-5.
49. Miao J, Amonette JE, Nishino Y, Ishikawa T, Hodgson KO. 2003. Direct determination of the absolute electron density of nanostructured and disordered materials at sub-10-nm resolution. *Phys. Rev. B* 68:012201.
50. Miao J, Hodgson KO, Ishikawa T, Larabell CA, LeGros MA, Nishino Y. 2003. Imaging whole Escherichia coli bacteria by using single-particle X-ray diffraction. *Proc. Natl. Acad. Sci. USA* 100:110-2.
51. Miao J, Hodgson KO, Sayre D. 2001. An approach to three-dimensional structures of biomolecules by using single-molecule diffraction images. *Proc. Natl. Acad. Sci., USA* 98:6641-5.
52. Millane RP. 1996. Multidimensional phase problems. *J. opt. Soc. Am A* 13:725-34.
53. Mozumder A. Charged particle tracks and their structure, in *Advances in Radiation Chemistry*, M. Burton and J. L. Magee, Eds. (Wiley, New York, 1969) pp. 1-102.
54. Neutze R, Wouts R, Spoel D, Weckert E, Hajdu J. 2000. Potential for biomolecular imaging with femtosecond X-ray pulses. *Nature* 406:752-57.
55. Pellegrini C. 1992. A 4 to 0.1 FEL Based on the SLAC Linac. In *Proceedings of the Workshop on 4th Generation Light Sources*, ed. M Cornacchia, H. Winick, pp. 376-84. SLAC, Stanford.
56. Phillips JC, Wlodawer A, Yevitz MM, Hodgson KO. 1976. Applications of Synchrotron Radiation to Protein Crystallography: Preliminary Results. *Proc. Natl. Acad. Sci. USA* 73:128-32.
57. Phillips JC, Wlodawer A, Goodfellow JM, Watenpaugh KD, Sieker LC, Jensen LH, Hodgson KO. 1977. Applications of Synchrotron Radiation to Protein Crystallography. II. Anomalous Scattering, Absolute Intensity, and Polarization. *Acta Cryst.* A33:445-55.
58. Robinson IK, Vartanyants IA, Williams GJ, Pferfer MA, Pitney JA. 2001. Reconstruction of the Shapes of Gold Nanocrystals Using Coherent X-ray Diffraction. *Phys. Rev. Lett.* 87:195505.
59. Rossmann MG, Blow DM. 1963. Determination of phases by the conditions of non-crystallographic symmetry. *Acta Crystallogr.* 16:39-45.
60. Sayre D. 1952. Implications of a theorem due to Shannon. *Acta Crystallogr.* 5:843.

61. Sayre D. in *Imaging Processes and Coherence in Physics. Springer Lecture Notes in Physics*, vol. 112, M. Schlenker *et al*., Eds. (Berlin: Springer, 1980) pp. 229-35.
62. Sayre D. in *Direct Methods of Solving Crystal Structures*, H. Schenck, Ed. (New York: Plenum, 1991), pp. 353-356.
63. Sayre D, Chapman H. 1995. X-ray microscopy. *Acta Crystallogr*. A51:237-252.
64. Sayre D, Chapman HN, Miao J. 1998. On the extendibility of X-ray crystallography to noncrystals. *Acta Crystallogr*. A 54:233-9.
65. Sayre D, Kirz J, Feder R, Kim DM, Spiller E. (1977). Transmission microscopy of unmodified biological materials: comparative radiation dosages with electrons and ultrasoft X-ray photons. *Ultramicroscopy* 2:337-41.
66. Schneider G. 1998. Cryo X-ray microscopy with high spatial resolution in amplitude and phase contrast. *Ultramicroscopy* 75:85-104.
67. Solem J, Baldwin GC. 1982. Microholography of living organisms. *Science* 218:229-235.
68. Spence JCH, Howells M, Marks LD, Miao J. 2001. Lensless imaging: a workshop on new approaches to the phase problem for non-periodic objects. *Ultramicroscopy* 90:1-6.
69. Spence JCH, Wu JS, Giacovazzo C, Carrozzini B, Cascarano GL, Padmore HA. 2003. Solving non-periodic structures using direct methods: phasing diffuse scattering. *Acta Crystallogr.* A 59:255-261.
70. Stroud RM, Agard DA. 1979. Structure determination of asymmetric membrane profiles using an iterative Fourier method. *Biophys. J.* 25:495-512.
71. Tigner M. 1965. A Possible Apparatus for Electron Clashing-Beam Experiments. *Nuovo Cimento* 37:1228-31.
72. Vartanyants IA, Robinson IK. 2001. Partial coherence effects on the imaging of small crystals using coherent X-ray diffraction. *J. Phys.: Condens. Matter* 13:10593-611.
73. Wang BC. 1985. Resolution of Phase Ambiguity in Macromolecular Crystallography. *Methods Enzymol.* 115:90-112.
74. Watenpaugh K, Smith J. eds. 1991. *Report of the Biological Synchrotron Users Organization (Biosync)*.
75. Weierstall U, Chen Q, Spence JCH, Howells MR, Isaacson M, Panepucci RR. 2001. Image reconstruction from electron and X-ray diffraction patterns using iterative algorithms: experiment and simulation. *Ultramicroscopy* 90:171-95.
76. Williams GJ, Pfeifer MA, Vartanyants IA, Robinson IK. 2003. Three-Dimensional Imaging of Microstructure in Au Nanocrystals. *Phys. Rev. Lett.* 90:175501.
77. Woolfson M, Fan HF. 1995. *Physical and non-physical methods of Solving Crystal Structures.* Cambridge: Cambridge University Press.
78. Yun W, Kirz J, Sayre D. 1987. Observation of the soft X-ray diffraction pattern of a single diatom. *Acta Crystallogr*. A 43:131-3.
79. Ziaja B, van der Spoel D, Szöke A, Hajdu J. 2001. Auger-electron cascades in diamond and amorphous carbon. *Phys. Rev. B* 64:214104.
80. Ziaja B, Szöke A, van der Spoel D, Hajdu J. 2002. Space-time evolution of electron cascades in diamond. *Phys. Rev. B* 66:024116.

81. Ziaja B, Szoke A, Hajdu J. 2002. Electron cascades produced by photoelectrons in diamond. arXiv:cond-mat/0208515v1

Figure Legends

Figure 1 Phase retrieval of an oversampled diffraction pattern recorded from a non-crystalline specimen. (a) A scanning electron microscopy image of the specimen. (b) An oversampled X-ray diffraction pattern of the specimen. (c) A specimen image as directly reconstructed from (b). (See ref. 44 for details)

Figure 2 (a) *E. coli* expressing the indicator protein. Individual bacteria are seen using transmitted light (A, D) and fluorescence (B, E), where the yellow fluorescence protein (green) is seen throughout most of the bacteria except for one small region in each bacterium that is free of fluorescence (arrows). C and F show the fluorescent image superimposed on the transmitted light image. (b) An oversampled X-ray diffraction pattern from the *E. Coli* bacteria. (c) An image reconstructed from (b). The dense regions inside the bacteria are likely the distribution of proteins labeled with $KMnO_4$. The semi-transparent regions are devoid of yellow fluorescence proteins, which are consistent with (a). (See ref. 50 for details)

Figure 3 An X-ray diffraction pattern from the yeast Saccharomyces cerevisiae. The pattern is a composite of several exposures, and displays the square root of the recorded diffraction intensity on a semi-log scale.

Figure 4 Peak brightness and x-ray pulse duration for a general class of "second" and "third" generation storage rings compared with that made possible from a next generation of linac-based sources. Also shown is a special type of "sliced" storage ring source, and example of which has recently become operational at the ALS in Berkeley. It can be seen that the ERLs/SPPS and XFELs offer the possibility of dramatic increases in per pulse brightness combined with much shorter pulse duration. The original concept for such a plot was given in conjunction with the Cornell proposal for an ERL (see ref. 22) and further elaborated in ref. 4.

Figure 5 A possible schematic layout for the experiment of imaging single biomolecules by using X-ray free electron lasers.

Figure 6 Structural determination of single rubisco molecules utilizing a simulated X-FEL and direct phase retrieval by the oversampling method. (a) Stereoview of the electron density map of the active site with a Mg(II) of the rubisco molecule (contoured at two sigma) on which the refined atomic model of the rubisco molecule is superimposed. The electron density map and the atomic model are obtained from protein data bank. (b) The active site reconstructed from a 3D diffraction pattern with R = 9.7%, on which the same atomic model is superimposed. (c) The reconstructed active site with R = 16.6%. (See ref. 51 for details)

Figures

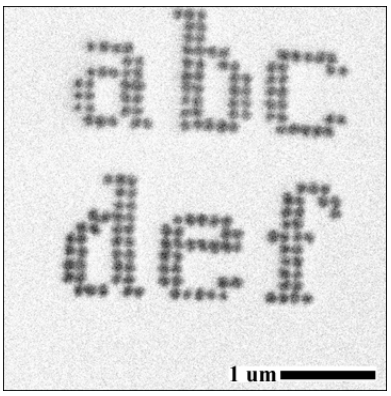

Figure 1(a)

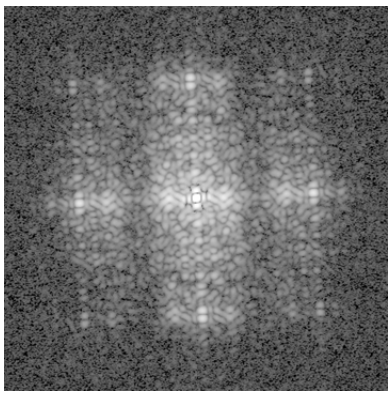

Figure 1(b)

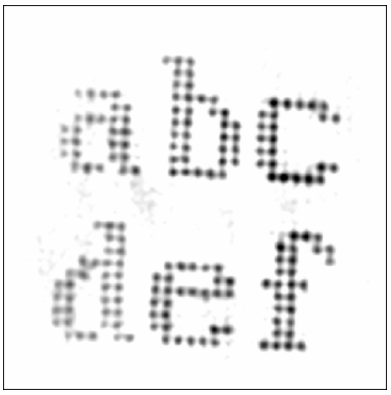

Figure 1(c)

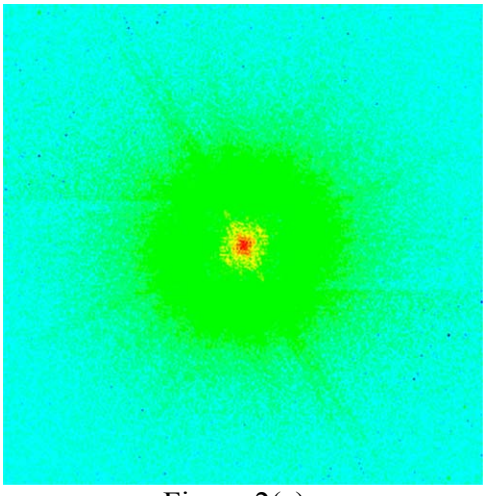

Figure 2(a)

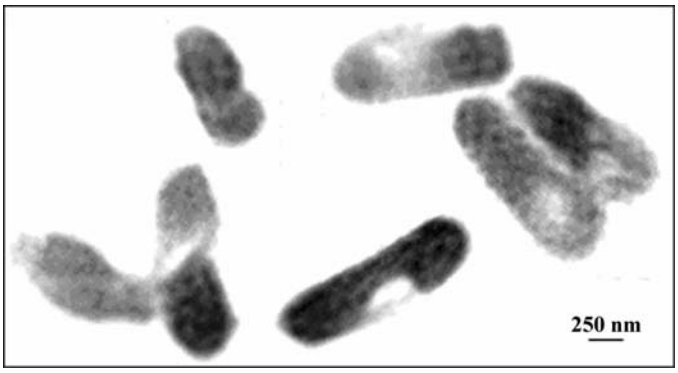

Figure 2(b)

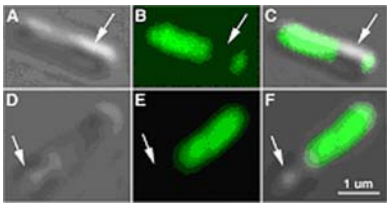

Figure 2(c)

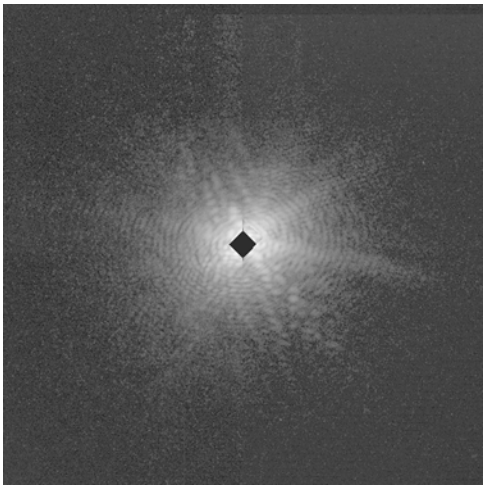

Figure 3

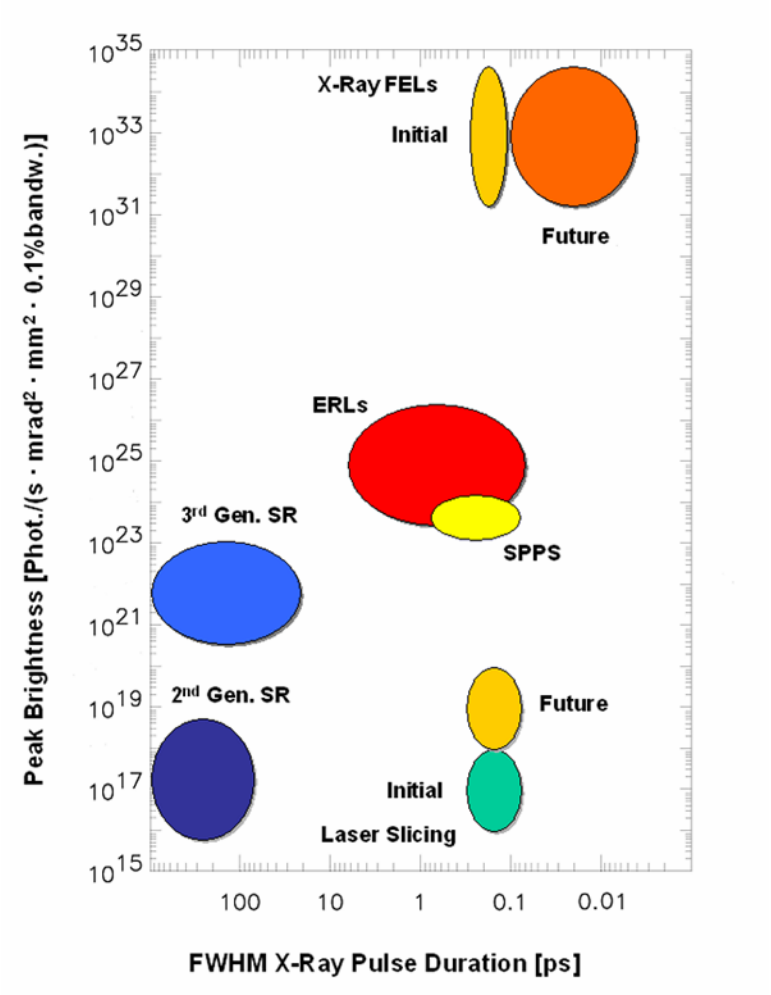

Figure 4

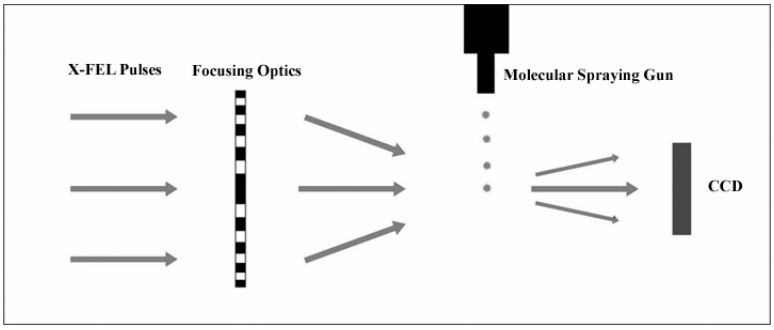

Figure 5

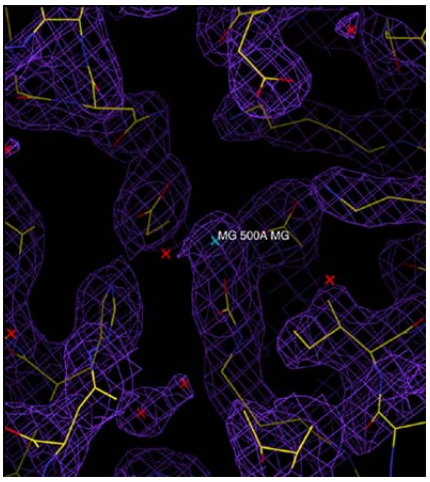

Figure 6(a)

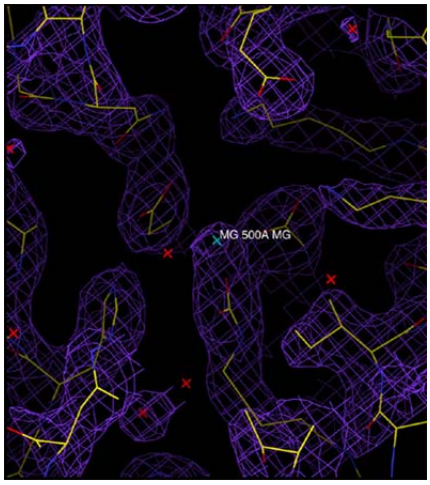

Figure 6(b)

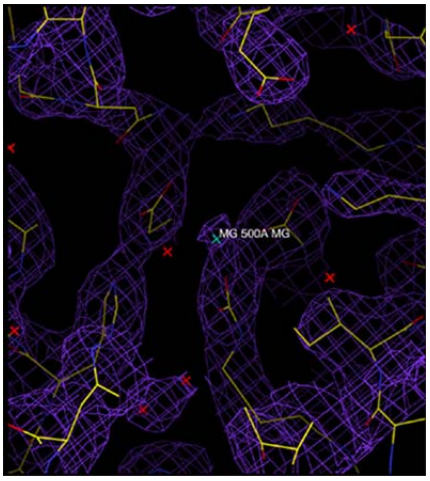

Figure 6(c)